Temporal and Spatial Variances in Arterial Spin-Labeling Are Inversely Related to Large-Artery Blood Velocity

A.D. Robertson, G. Matta, V.S. Basile, S.E. Black, C.K. Macgowan, J.A. Detre, and B.J. MacIntosh

ABSTRACT

BACKGROUND AND PURPOSE: The relationship between extracranial large-artery characteristics and arterial spin-labeling MR imaging may influence the quality of arterial spin-labeling–CBF images for older adults with and without vascular pathology. We hypothesized that extracranial arterial blood velocity can explain between-person differences in arterial spin-labeling data systematically across clinical populations.

MATERIALS AND METHODS: We performed consecutive pseudocontinuous arterial spin-labeling and phase-contrast MR imaging on 82 individuals (20–88 years of age, 50% women), including healthy young adults, healthy older adults, and older adults with cerebral small vessel disease or chronic stroke infarcts. We examined associations between extracranial phase-contrast hemodynamics and intracranial arterial spin-labeling characteristics, which were defined by labeling efficiency, temporal signal-to-noise ratio, and spatial coefficient of variation.

RESULTS: Large-artery blood velocity was inversely associated with labeling efficiency ($P = .007$), temporal SNR ($P < .001$), and spatial coefficient of variation ($P = .05$) of arterial spin-labeling, after accounting for age, sex, and group. Correction for labeling efficiency on an individual basis led to additional group differences in GM-CBF compared to correction using a constant labeling efficiency.

CONCLUSIONS: Between-subject arterial spin-labeling variance was partially explained by extracranial velocity but not cross-sectional area. Choosing arterial spin-labeling timing parameters with on-line knowledge of blood velocity may improve CBF quantification.

ABBREVIATIONS: ASL = arterial spin-labeling; CoV = coefficient of variation; PC = phase contrast; WMH = white matter hyperintensities

Quantitative CBF is a valuable measure to track pathophysiologic changes in cerebrovascular function and brain metabolism.[1] Two noninvasive MR imaging–based techniques, which capture distinct hemodynamic features, are arterial spin-labeling (ASL) and phase-contrast (PC) imaging. ASL measures regional CBF with tissue-level precision, using magnetized arterial blood water as an endogenous tracer.[2,3] PC imaging, by comparison, quantifies whole-brain CBF with a bipolar gradient to induce phase shifts proportional to blood velocity within the carotid and vertebral arteries.[4] Among the factors that influence ASL, CBF quantification is most sensitive to labeling efficiency and the equilibrium magnetization of arterial blood.[5] In practice, labeling efficiency is assumed constant (eg, 0.85).[3] Field inhomogeneity[6] and nonlinear effects of blood velocity,[7-9] however, contribute individual variability. Studies that have empirically estimated labeling efficiency by normalizing pseudocontinuous ASL-based whole-brain CBF to that measured with PC imaging report individual labeling efficiencies ranging from 0.7 to 1.1.[8,10] Recent work in a large middle-aged cohort, however, has questioned the validity of this normalization method due to substan-

Received October 28, 2016; accepted after revision April 10, 2017.

From the Heart and Stroke Foundation Canadian Partnership for Stroke Recovery (A.D.R., G.M., S.E.B., B.J.M.) and Hurvitz Brain Sciences (A.D.R., S.E.B., B.J.M.), Sunnybrook Research Institute, University of Toronto, Toronto, Ontario, Canada; Division of Neurology, Department of Medicine (V.S.B., S.E.B.), University of Toronto, Toronto, Ontario, Canada; Mackenzie Health (V.S.B.), Richmond Hill, Ontario, Canada; L.C. Campbell Cognitive Neurology Research Unit (S.E.B.), Sunnybrook Health Sciences Centre, Toronto, Ontario, Canada; Hospital for Sick Children (C.K.M.), Toronto, Ontario, Canada; Department of Medical Biophysics (C.K.M., B.J.M.), University of Toronto, Toronto, Ontario, Canada; and Department of Neurology (J.A.D.), University of Pennsylvania, Philadelphia, Pennsylvania.

This work was supported by a research grant from the Canadian Institutes of Health Research (MOP133568) and catalyst grants from the Heart and Stroke Foundation Canadian Partnership for Stroke Recovery.

Paper previously presented, in part, as a poster at: Annual Meeting and Exhibition of the International Society for Magnetic Resonance in Medicine, May 30 to June 5, 2015; Toronto, Ontario, Canada. G. Matta, A.D. Robertson, S.E. Black, and B.J. MacIntosh. "Quantifying Cerebral Blood Flow: A Comparison of Two Noninvasive Perfusion Imaging Techniques."

Please address correspondence to Andrew Robertson, PhD, Heart and Stroke Foundation Canadian Partnership for Stroke Recovery, Sunnybrook Research Institute, Rm M6–168, 2075 Bayview Ave, Toronto, ON, Canada, M4N 3M5; e-mail: adrobert@sri.utoronto.ca; @arob888

http://dx.doi.org/10.3174/ajnr.A5257

tial variability within individual measurements.[11] Rather than incorporating PC-based CBF as a normalization factor, corresponding knowledge of PC-based metrics, such as blood velocity, may be beneficial for planning ASL protocols because many labeling and acquisition parameters are timing-based.

Simulated and empiric ASL data suggest that labeling efficiency is highest for blood velocities of ~10 cm/s.[8] These studies reflect hemodynamics in healthy adults, leaving questions regarding the reliability of ASL in patients with vascular pathology. Aging, cerebrovascular risk factors, and stroke status are associated with larger cross-sectional areas and slower, more pulsatile blood velocity within the large arteries.[12,13] Such changes occurring in proximity to the ASL labeling plane may confound CBF quantification in these clinical cohorts. For instance, age is associated with a decreased signal-to-noise ratio, due, in part, to increased variance between individual control-tag difference images.[14] Arterial transit time is another velocity-sensitive hemodynamic characteristic associated with aging[15] and the presence of white matter hyperintensities (WMH).[16] Prolonged transit time is visualized by localized regions of hyperintense ASL signal, contributing to greater spatial variance in whole-brain CBF.[17] To expand our understanding of the relationship between large-artery characteristics and CBF estimates, we compared ASL and PC in individuals across a range of age and vascular pathology. We hypothesized that large-artery blood velocity would be inversely related to labeling efficiency, temporal SNR, and spatial variance in ASL.

MATERIALS AND METHODS

Participants and Protocol

Participants were recruited into 4 groups: 1) healthy young adults (younger than 40 years); 2) healthy older adults (50 years or older); 3) older adults with WMH of presumed vascular origin; and 4) older adults with chronic stroke infarcts (≥3 months post-stroke). Exclusion criteria included the presence of dementia, a genetic predisposition to WMH, and extracranial arterial occlusion. Participants underwent a single MR imaging scan. The Sunnybrook Research Institute's research ethics board approved this study, and all participants provided written informed consent.

MR Imaging Acquisition

We completed neuroimaging with a 3T MR imaging system (Achieva; Philips Healthcare, Best, the Netherlands) with a body coil transmitter and an 8-channel head coil receiver. Structural imaging included high-resolution T1 (TR/TE = 9.5/2.3 ms, flip angle = 8°, voxel dimensions = 0.9 × 0.7 × 1.2 mm^3, FOV = 240 × 191 × 168 mm^3) and FLAIR (TR/TE/TI = 9000/125/2800 ms, flip angle = 90°, voxel dimensions = 0.4 × 0.4 × 3 mm^3, FOV = 240 × 240 × 156 mm^3) acquisitions. Two 2D acquisitions independently quantified CBF: PC to measure large-artery blood flow and ASL to measure tissue-level CBF. The PC acquisition captured a single 5-mm section perpendicular to the extracranial internal carotid artery, with cardiac synchronization (finger pulse gating, single cardiac phase [acquisition delay = 250 ms, acquisition window = 500 ms], TR/TE = 20/9.1 ms, flip angle = 15°, maximum velocity encoding = 100 cm/s, voxel dimensions = 0.5 × 0.5 mm^2, FOV = 150 × 150 mm^2). Pseudocontinuous labeling for the ASL scan used a train of radiofrequency pulses (duration = 0.5 ms, flip angle = 18°, interpulse pause = 0.5 ms) with a balanced gradient scheme for 1650 ms and occurred at a position identical to that of the PC acquisition. Thirty control and tag ASL volume pairs were acquired by single-shot echo-planar imaging (TR/TE = 4000/9.6 ms, flip angle = 90°, in-plane resolution = 3 × 3 mm^3, FOV = 192 × 192 mm^3, section thickness = 5 mm, number of sections = 18 [no gap], postlabel delay = 1600 ms at the first section and ascending for subsequent sections).

We did not select background suppression to maximize the detectability of deleterious individual-difference images that were spurious due to head motion. A proton density–weighted reference volume was acquired to estimate the equilibrium magnetization and extract a receiver coil sensitivity profile (TR = 10 seconds, but otherwise identical to ASL parameters). We prioritized the frontal cortices and subcortical tissue when setting the ASL FOV, leaving inconsistent coverage of the cerebellum and the most superior cerebrum. PC and ASL scan durations were 1.5 and 4.5 minutes, respectively. The 2 acquisitions were run sequentially, and the order was varied between participants.

MR Imaging Processing

Images were processed with the FMRIB Software Library (FSL; www.fmrib.ox.ac.uk/fsl). Brain extraction[18] and segmentation[19] tools isolated GM and WM from the T1WI. Brain mass was estimated on the basis of tissue densities of 1.03 g/mL for GM and 1.04 g/mL for WM.[20] In-house software,[21] combined with manual editing, segmented WMH from the FLAIR image. Stroke lesions were identified by CSF segmentation from the T1WI, manual editing, and confirmation against the FLAIR image. WMH and infarct volumes were normalized to an intracranial capacity of 1300 mL. Older adults with a normalized hyperintensity burden of ≥10 mL across periventricular and deep brain regions were assigned to the WMH group.

Internal carotid and vertebral artery masks were isolated from the PC magnitude image by using FSL segmentation software and manual editing. Interrater reliability of this method was excellent (Cronbach α >0.99 for the internal carotid artery and >0.95 for the vertebral artery between 1 experienced and 2 novice raters). These masks represent the cross-sectional area of each artery, and they were overlaid onto the PC phase image to compute mean blood velocity. Arterial blood flow is the product of area and mean velocity, and PC-CBF was calculated as the sum of flow through all 4 arteries, normalized to brain mass. Peak blood velocity was taken as the highest velocity signal from a voxel in the center of the vessel lumen.

ASL-CBF was calculated from the mean of the control-tag difference images. To maximize image quality, we systematically removed individual-difference images with high relative head motion before CBF calculation, as previously described.[14] The remaining difference images underwent in-plane spatial smoothing by using a Gaussian kernel of 5-mm full width at half maximum, section-by-section adjustment for incremental postlabel delay, and calibration to absolute CBF units with a proton density–weighted image.[3] The T1 relaxation time for arterial blood was set at 1.65 seconds for all participants. Calibration to absolute CBF units at this stage did not correct for labeling efficiency. Images with intravascular artifacts were retained. Although intravas-

Table 1: Participant characteristics[a]

	Young	Old	WMH	Stroke	*P* Value
No.	15	22	15	30	
Age (range) (yr)	25.7 ± 4.6 (20–36)	69.1 ± 7.0[b] (55–81)	72.0 ± 8.2[b] (51–83)	67.9 ± 10.4[b] (51–88)	<.001
Sex, female (%)	7 (47)	17 (77)	8 (53)	9 (30)	.009
Hemodynamics					
ICA mean velocity (cm/s)	18.2 ± 4.5	11.9 ± 2.9[b]	10.3 ± 3.3[b]	9.7 ± 3.1[b]	<.001
ICA area (cm^2)	0.21 ± 0.04	0.24 ± 0.06	0.26 ± 0.06	026 ± 0.09	.102
VA mean velocity (cm/s)	10.0 ± 2.5	6.7 ± 1.6[b]	6.5 ± 1.7[b]	5.6 ± 2.1[b]	<.001
VA area (cm^2)	0.13 ± 0.03	0.13 ± 0.03	0.14 ± 0.04	0.12 ± 0.03	.190
PC-CBF (mL/100 g/min)	49.0 ± 8.5	41.4 ± 8.1	40.6 ± 12.9	33.8 ± 6.3[b,c]	<.001
ASL-CBF (mL/100 g/min)	44.1 ± 10.2	40.8 ± 8.8	31.4 ± 9.6[b,c]	34.3 ± 10.5[b]	<.001

Note:—VA indicates vertebral artery.

[a] Data are mean ± SD or count (proportion). Area and velocity are reported as the mean of bilateral vessels. ASL-CBF is uncorrected for labeling efficiency.

[b] Group differences compared with the young group at $P_{Bonferroni} < .05$.

[c] Group differences compared with the old group at $P_{Bonferroni} < .05$.

cular artifacts are suggestive of prolonged arterial transit time, CBF calculations over the whole brain should remain valid in the absence of crushing gradients.[3]

We calculated 4 ASL variables to compare against extracranial hemodynamics: 1) GM-CBF, 2) individual labeling efficiency equal to the ratio between ASL-based and PC-based whole-brain CBF, 3) temporal SNR equal to the ratio between the mean and the SD of the individual-difference images, and 4) spatial coefficient of variation (CoV) equal to the ratio between the SD and mean of the GM-CBF image. A GM mask without any overlapping stroke lesion was created for the calculation of GM-CBF, temporal SNR, and spatial CoV. GM-CBF was subsequently corrected for labeling efficiency in 2 ways: 1) with a constant of 0.85, and 2) with the calculated labeling efficiency.

Statistical Analysis

CBF, mean blood velocity, and cross-sectional area were compared between groups by ANOVA. We assessed the associations of mean blood velocity and cross-sectional area with GM-CBF, individual labeling efficiency, temporal SNR, and spatial CoV by linear regressions, adjusting for age, sex, and group. To account for between-vessel differences in area and velocity, we calculated flow-weighted measures in which the influence of each artery on the pooled variables was proportional to the contribution of that vessel to whole-brain CBF. Differences between whole-brain ASL-CBF and PC-CBF were characterized in a paired analysis by ratio and mean difference. Finally, we compared GM-CBF with the 2 distinct labeling efficiencies. Unpaired *t* tests with Bonferroni correction ($P_{Bonferroni}$) were used for post hoc group comparisons. All statistical analyses were performed with R statistical and computing software (Version 3.3.1; http://www.r-project.org/), with $P < .05$ being significant.

RESULTS

Large-artery characteristics and whole-brain hemodynamics from 82 participants ($n = 15$ young, 22 healthy older, 15 with WMH, and 30 with stroke) are reported in Table 1. In WMH, the normalized hyperintensity volume ranged from 10.9 to 52.2 mL. Stroke participants were 3–65 months postevent with cortical, subcortical, and subtentorial infarcts. The normalized infarct volume ranged from 0.03 to 98.2 mL. Group differences in velocity, but not cross-sectional area, were observed (Fig 1). Although the fraction of whole-brain CBF contributed by each extracranial artery was similar across groups, greater within-group variability was observed in older adults with vascular pathology (Fig 1, lower panel).

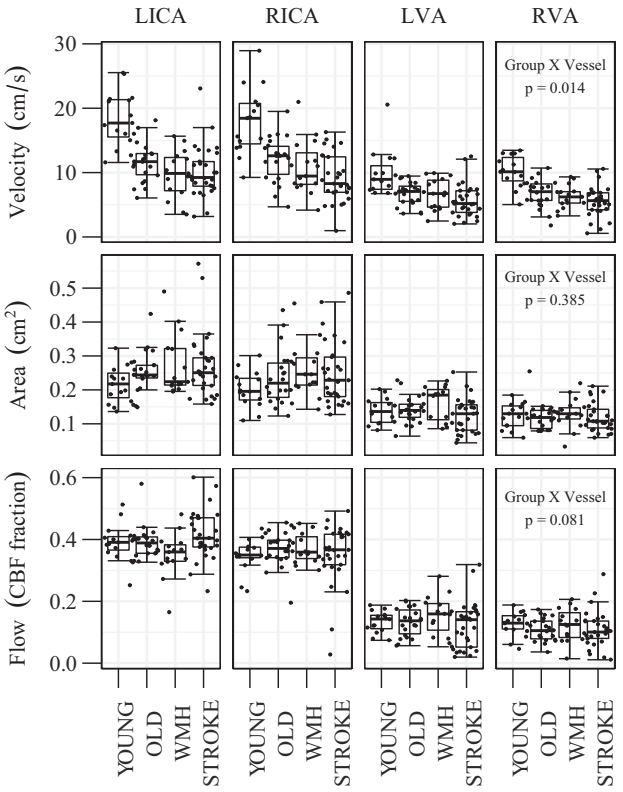

FIG 1. Vascular characteristics of the bilateral (left and right) internal carotid (LICA and RICA) and vertebral arteries (LVA and RVA) for each group. Panel 3 shows the relative contribution to total CBF by each vessel.

Labeling Efficiency

PC-CBF accounted for a significant proportion of the between-person variance in ASL-CBF ($r^2 = 0.40$, $P < .001$), though technique differences were evident. Intermodality analyses suggested that ASL-CBF was systematically lower than PC-CBF ($t = -2.6$, $P = .01$), and this difference was greater in WMH than in stroke or healthy older adults groups (Table 2). The ASL-CBF to PC-CBF ratio (ie, individual labeling efficiency) ranged from 0.48 to 1.60 across our entire sample. A group effect was observed ($F = 4.3$, $P = .008$), with the ratio being lower in WMH than in stroke and

Table 2: Comparison of MRI methods for whole-brain CBF estimation[a]

	No.	ASL:PC (ratio)	ASL-PC Difference (mL/100 g/min)
Young	15	0.91 ± 0.20	−4.9 ± 9.8
Old	22	1.00 ± 0.18[b]	−0.6 ± 7.0[b]
WMH	15	0.80 ± 0.20	−9.2 ± 9.4
Stroke	30	1.01 ± 0.23[b]	0.5 ± 7.9[b]
All	82	0.95 ± 0.22	−2.6 ± 9.0

[a] Data are mean ± SD.

[b] Group differences compared with WMH at $P_{Bonferroni} < .05$.

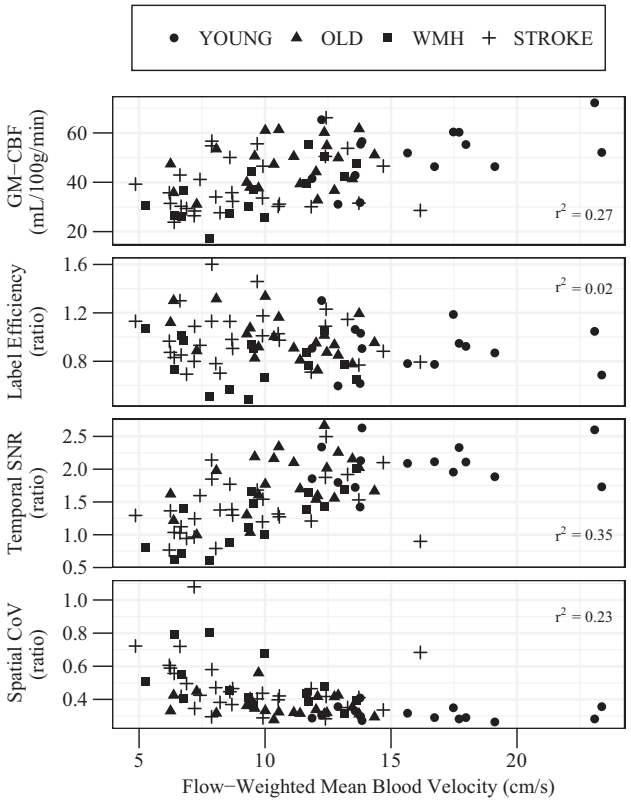

FIG 2. The association of mean blood velocity with GM-CBF (panel 1), ASL-to-PC ratio for whole-brain CBF (panel 2), ASL temporal SNR (panel 3), and CBF spatial CoV (panel 4). Velocity is shown as a weighted mean of all 4 extracranial vessels relative to their contribution to total CBF. GM-CBF is uncorrected for labeling efficiency. Age, sex, and group-adjusted linear models are reported in Table 3.

healthy older adults groups. Labeling efficiency was unrelated to mean blood velocity in bivariate linear regression (Fig 2), though labeling efficiency and peak blood velocity showed a modest correlation ($r^2 = 0.05$, $P = .043$). Furthermore, an inverse association between labeling efficiency and mean velocity was observed in a regression model that adjusted for age, sex, group status, and cross-sectional area (Table 3). This multivariate model was unaltered when peak velocity replaced mean velocity.

Temporal and Spatial Variance

Group differences in the temporal SNR within gray matter were observed (young: 2.05 ± 0.33 versus old: 1.79 ± 0.43 versus WMH: 1.23 ± 0.44 versus stroke: 1.42 ± 0.42; $F = 13.4$, $P < .001$). No difference between young and healthy older adults was noted, but both groups had greater SNR than WMH and stroke groups ($P_{Bonferroni} \leq 0.010$). Group differences in spatial CoV within gray matter were also observed (young: 0.31 ± 0.04 versus old: 0.36 ± 0.07 versus WMH: 0.49 ± 0.15 versus stroke: 0.48 ± 0.16; $F = 8.80$, $P < .001$). Again, no difference between young and healthy older adults was noted, but both groups exhibited less spatial CoV than WMH and stroke groups ($P_{Bonferroni} < .05$). Both temporal SNR and spatial CoV were associated with mean blood velocity in bivariate analysis (Fig 2) and remained significant after adjusting for age, sex, and group (Table 3). The spread of spatial CoV increased with decreasing velocity, particularly below 10 cm/s. Calculated label efficiency was directly related to temporal SNR ($r^2 = 0.07$, $P = .017$), but not spatial CoV ($r^2 = 0.02$, $P = .16$).

GM-CBF

GM-CBF was directly correlated with mean blood velocity (Fig 2 and Table 3). A group-by-method interaction ($F = 4.6$, $P = .005$) indicated that additional group differences in GM-CBF were observed when using a PC-based correction for labeling efficiency compared with the constant 0.85 correction (Fig 3). When we used the constant correction across all participants, GM-CBF was lower in the WMH and stroke groups than in young adults and lower in the WMH group than in healthy older adults. Correction for PC-based labeling efficiency identified additional differences between the healthy young and old groups and between the healthy old and stroke groups.

DISCUSSION

The accuracy of regional CBF maps—an important consideration for the clinical uptake of ASL imaging—depends on multiple parameters in the scanning protocol. In this study, we compared PC and ASL MR imaging in adults with and without vascular-related pathology to assess how large-artery characteristics relate to ASL signal. The regression results demonstrated an inverse relationship between labeling efficiency and arterial blood velocity, which is consistent with previous work.[8] However, label efficiency variance was high for low velocities; thus, we are unable to provide empiric support for the theorized inverted U-shaped profile.[7-9] Notably, features of ASL variance, namely temporal SNR and spatial CoV, were independently associated with mean blood velocity but not cross-sectional area in regression analyses. Reduced temporal SNR at a low velocity contributed to the increased variance of labeling efficiency within this range. These results reaffirm that hemodynamics at the labeling plane are an important consideration for CBF quantification in ASL, especially in older adults with cerebrovascular disease.

Previous work estimated ASL labeling efficiency based on PC,[7-9] though the validity of this method has recently come under scrutiny.[11] Our current findings contrast with ASL simulations that posited a direct association between velocity and labeling efficiency below peak velocities of 20 cm/s.[7,9] Whereas the previous findings were under the assumption of constant flow profiles, our PC implementation averaged velocities over the cardiac cycle; consequently, the velocity estimates more closely reflect data from Aslan et al,[8] who found an inverse association between velocity and labeling efficiency above 10 cm/s. ASL signal intensity and transit delays have been shown to vary as a function of the cardiac cycle,[22] so dissimilar relationships between mean and peak veloc-

Table 3: Linear regression parameters for the association of extracranial mean blood velocity and cross-sectional area with ASL characteristics[a]

Model	Independent Variables	β	95% CI	*T*-Statistic	*P* Value
GM-CBF	Area (cm^2)	46.5	(8.2–84.7)	2.03	.046
Adjusted $R^2 = 0.43$	Velocity (cm/s)	1.5	(0.8–2.3)	3.42	.001
ASL-CBF:PC-CBF	Area (cm^2)	−0.79	(−1.58–0.01)	−1.65	.103
Adjusted $R^2 = 0.21$	Velocity (cm/s)	−0.02	(−0.04–0.01)	−2.78	.007
GM-temporal SNR	Area (cm^2)	1.78	(0.24–3.32)	1.93	.058
Adjusted $R^2 = 0.47$	Velocity (cm/s)	0.07	(0.04–0.10)	3.99	<.001
GM-spatial CoV	Area (cm^2)	−0.11	(−0.61–0.39)	−0.36	.720
Adjusted $R^2 = 0.31$	Velocity (cm/s)	−0.01	(−0.02–0.00)	−2.01	.048

[a] All models were adjusted for age, sex, and group. GM-CBF is uncorrected for labeling efficiency.

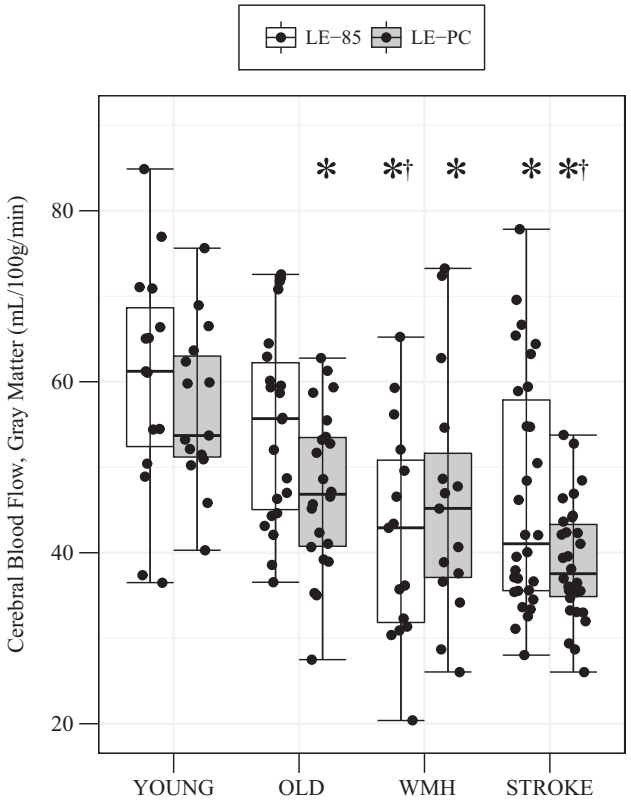

FIG 3. GM-CBF between groups calculated with 2 labeling efficiency estimates. *White bars* incorporate a constant labeling efficiency (ie, 0.85), and *gray bars* incorporate individual labeling efficiency based on the ASL-to-PC ratio for whole-brain CBF. Post hoc group comparisons are indicated at $P_{Bonferroni} < .05$ for differences from the young group (*asterisk*) and differences from old group (*dagger*) within the same calibration technique.

ity may reflect temporal fluctuations in effective labeling efficiency. Of note, we found labeling efficiency to be more sensitive to peak velocity than mean velocity in unadjusted models.

In addition to labeling efficiency, the temporal and spatial variability of ASL signal were inversely related to mean blood velocity. At labeling, the volume of labeled blood is a function of blood velocity and label duration, the latter of which was held constant at 1650 ms. Intuitively, lower velocities will degrade ASL because the label volume directly translates to signal-to-noise ratio.[3] At acquisition, ASL signal is dependent on the arterial transit time and the T1 relaxation of arterial blood.[23] Arterial transit time increases with cerebrovascular disease.[24,25] Thus, labeled blood is more likely to remain in the macrovascular compartment and be captured as hyperintense signal, contributing to greater heterogeneity within the perfusion-weighted image.[26] Indeed, a recent ASL study in hypertensive older adults demonstrated a direct relationship between single postlabel delay spatial CoV and arterial transit time.[17] To combat this, longer postlabel delays are recommended for imaging older adults to allow signal to reach the tissue before acquisition, albeit at a cost of lower signal intensity.[3] We observed that slower velocity was related to greater spatial CoV of the perfusion-weighted image, which is consistent with greater macrovascular signal at the time of acquisition. Real-time monitoring of blood velocity before ASL planning may help mitigate these indices of ASL variance in 2 ways: First, acquiring additional tag and control volumes in individuals with low velocity would improve signal-to-noise ratio. Second, prescribing postlabel delay based on arterial blood velocity may help to distinguish aspects of arterial transit time that separate slower flow velocity from collateral or tortuous pathways.

The GM-CBF values observed here are consistent with those in other studies involving younger adults,[27] healthy older adults,[28] and individuals with chronic stroke.[29] Older adults with WMH, however, exhibited lower GM-CBF than previously reported.[30] Calibration of the GM-CBF to individual labeling efficiency on the basis of PC altered the sensitivity to distinguish clinical groups. With PC-based calibration, we noted GM-CBF differences between healthy young and older adults and between healthy older adults and those with stroke, which were not apparent with a constant labeling efficiency for all participants. Longitudinal relaxation time was held constant across all groups in our estimation of CBF with ASL. Age- and sex-dependent variability in blood T1 may have partially contributed to group differences in global ASL signal.[31] The change in group differences following calibration to PC-CBF, which is independent of blood T1 effects, may be partially due to correction for group differences in longitudinal relaxation. Nevertheless, these results raise important questions about the consideration of labeling efficiency and the design of ASL protocols for CBF quantification in clinical cohorts with altered large-artery velocity profiles.

Despite these proposed links between blood velocity and ASL, a large proportion of the variance remains unexplained in this study. In several cases, the calculated labeling efficiency exceeded 1.0, which is an implausible finding. We implemented gated cardiac PC-MRI to capture velocity data at a single phase in the cardiac cycle on the basis of a 500-ms acquisition window that was optimized for a range of R-R intervals centered at 1000 ms. Heart rate variability could shift this acquisition window to favor the diastolic phase of the cardiac cycle, which would influence the PC-CBF calculation and contribute to a higher ratio between ASL-CBF and PC-CBF. Vessel segmentation and partial volume errors related to vertebral artery tortuosity[32] and smaller arterial caliber may have reduced PC-CBF accuracy.[33] Another consideration is the ASL volume coverage. Whereas PC-CBF reflects whole-brain flow, the ASL FOV did not encapsulate the entire

brain for all participants. Anatomic variability in the circle of Willis (ie, distal to PC imaging) may also contribute to a mismatch between upstream and downstream flow measurements.[34]

These discrepancies may have contributed to a portion of the unexplained variance between ASL-CBF and PC-CBF and emphasize the need for caution when comparing ASL-CBF directly with PC-CBF.[11] Of note, our ASL protocol did not incorporate background suppression or involve 3D acquisition, which are now consensus guidelines for clinical ASL.[3] Two main reasons for these preferences were the following: 1) Study development predated the consensus article, and 2) a parallel objective of the data acquisition was to address deleterious head motion, which is more easily approached with multiple 2D sections as opposed to 3D readouts. Recently, a sequence that measures artery-specific label efficiency, thereby improving ASL-CBF accuracy, has been proposed and validated.[35] Comparison of PC-CBF with ASL-CBF using this calibration method may facilitate investigation into the impact of age- and disease-related increases in hemodynamic pulsatility on ASL after controlling for effects on label efficiency.

CONCLUSIONS

The current study compared characteristics from ASL- and PC-based cerebral perfusion imaging in adults with and without vascular disease. Mean blood velocity through the ASL labeling plane was inversely related to labeling efficiency, as well as ASL temporal and spatial variance. These associations suggest that velocity impacts ASL at both the labeling and acquisition stages. ASL planning based on real-time velocity monitoring (eg, number of control/tag pairs, postlabel delay) may help optimize the signal-to-noise ratio and minimize the effect of arterial transit time on CBF maps.

ACKNOWLEDGMENTS

The authors thank Dr Henk-Jan Mutsaerts for valuable discussions regarding this work and MR imaging technologists, Ms. Ruby Endre and Mr Garry Detzler, for their assistance with data collection.

Disclosures: Sandra E. Black—*UNRELATED*: *Consultancy*: Novartis, Merck, Pfizer, Eli Lilly, *Comments*: ad hoc consulting; *Grants/Grants Pending*: Hoffmann-La Roche, Eli Lilly, Pfizer, Lundbeck, Transition Therapeutics, GE Healthcare, Axovant Sciences, Cognoptix, Biogen, Canadian Institutes of Health Research, National Institutes of Health, Heart and Stroke Foundation of Canada, Alzheimer's Drug Discovery Foundation, Brain Canada, Ontario Brain Institute, Fondation Leducq, Weston Foundation, Canadian Partnership for Stroke Recovery, *Comments*: contract grants and grants from government agencies paid to the institution*; *Payment for Lectures Including Service on Speakers Bureaus*: Medscape, Biogen, *Comments*: lecture presented at the Alzheimer's Association International Conference, 2016, Toronto. John A. Detre—*UNRELATED*: *Board Membership*: International Society for Magnetic Resonance in Medicine, *Comments*: board member, 2011–2014; *Consultancy*: Child Health and Development Institute, Ironwood Pharmaceuticals, National Institutes of Health, Wellcome Trust, *Comments*: I have been a paid consultant on neuroimaging for the Child Health and Development Institute (nonprofit Huntington disease research entity, Ironwood Pharmaceuticals company); I review grants for National Institutes of Health and the Wellcome Trust (UK) and have received honoraria for that work; *Employment*: University of Pennsylvania; *Grants/Grants Pending*: National Institutes of Health, *Comments*: I am a co-investigator on numerous National Institutes of Health grants that are funded or pending*; *Payment for Lectures Including Service on Speakers Bureaus*: Stanford University, Moss Rehabilitation Research Institute, Korean Society for Magnetic Resonance in Medicine; *Stock/Stock Options*: Blackfynn, *Comments*: I am eligible for stock in Blackfynn, a Pennsylvania startup company in exchange for consulting, but I have not exercised this option. *Money paid to the institution.

REFERENCES

1. Detre JA, Wang J, Wang Z, et al. **Arterial spin-labeled perfusion MRI in basic and clinical neuroscience.** *Curr Opin Neurol* 2009;22:348–55 CrossRef Medline
2. Williams DS, Detre JA, Leigh JS, et al. **Magnetic resonance imaging of perfusion using spin inversion of arterial water.** *Proc Natl Acad Sci U S A* 1992;89:212–16 CrossRef Medline
3. Alsop DC, Detre JA, Golay X, et al. **Recommended implementation of arterial spin-labeled perfusion MRI for clinical applications: a consensus of the ISMRM perfusion study group and the European consortium for ASL in dementia.** *Magn Reson Med* 2015;73:102–16 CrossRef Medline
4. Bakker CJ, Hoogeveen RM, Viergever MA. **Construction of a protocol for measuring blood flow by two-dimensional phase-contrast MRA.** *J Magn Reson Imaging* 1999;9:119–27 Medline
5. Wu WC, St. Lawrence KS, Licht DJ, et al. **Quantification issues in arterial spin labeling perfusion magnetic resonance imaging.** *Top Magn Reson Imaging* 2010;21:65–73 CrossRef Medline
6. Jahanian H, Noll DC, Hernandez-Garcia L. **B0 field inhomogeneity considerations in pseudo-continuous arterial spin labeling (pCASL): effects on tagging efficiency and correction strategy.** *NMR Biomed* 2011;24:1202–09 CrossRef Medline
7. Dai W, Garcia De Bazelaire C, et al. **Continuous flow-driven inversion for arterial spin labeling using pulsed radio frequency and gradient fields.** *Magn Reson Med* 2008;60:1488–97 CrossRef Medline
8. Aslan S, Xu F, Wang PL, et al. **Estimation of labeling efficiency in pseudocontinuous arterial spin labeling.** *Magn Reson Med* 2010;63:765–71 CrossRef Medline
9. O'Gorman RL, Summers PE, Zelaya FO, et al. **In vivo estimation of the flow-driven adiabatic inversion efficiency for continuous arterial spin labeling: a method using phase contrast magnetic resonance angiography.** *Magn Reson Med* 2006;55:1291–97 CrossRef Medline
10. Vidorreta M, Wang Z, Rodríguez I, et al. **Comparison of 2D and 3D single-shot ASL perfusion fMRI sequences.** *Neuroimage* 2013;66:662–71 CrossRef Medline
11. Dolui S, Wang Z, Wang DJ, et al. **Comparison of noninvasive MRI measurements of cerebral blood flow in a large multisite cohort.** *J Cereb Blood Flow Metab* 2016;36:1244–56 CrossRef Medline
12. Bai CH, Chen JR, Chiu HC, et al. **Lower blood flow velocity, higher resistance index, and larger diameter of extracranial carotid arteries are associated with ischemic stroke independently of carotid atherosclerosis and cardiovascular risk factors.** *J Clin Ultrasound* 2007;35:322–30 CrossRef Medline
13. Homma S, Sloop GD, Zieske AW. **The effect of age and other atherosclerotic risk factors on carotid artery blood velocity in individuals ranging from young adults to centenarians.** *Angiology* 2009;60:637–43 CrossRef Medline
14. Shirzadi Z, Crane DE, Robertson AD, et al. **Automated removal of spurious intermediate cerebral blood flow volumes improves image quality among older patients: a clinical arterial spin labeling investigation.** *J Magn Reson Imaging* 2015;42:1377–85 CrossRef Medline
15. Liu Y, Zhu X, Feinberg D, et al. **Arterial spin labeling MRI study of age and gender effects on brain perfusion hemodynamics.** *Magn Reson Med* 2012;68:912–22 CrossRef Medline
16. Nasel C, Boubela R, Kalcher K, et al. **Normalised time-to-peak-distribution curves correlate with cerebral white matter hyperintensities: could this improve early diagnosis?** *J Cereb Blood Flow Metab* 2017;37:444–55 CrossRef Medline
17. Mutsaerts HJ, Petr J, Václavů L, et al. **The spatial coefficient of variation in arterial spin labeling cerebral blood flow images.** *J Cereb Blood Flow Metab* 2017 Jan 1. [Epub ahead of print] CrossRef Medline
18. Smith SM. **Fast robust automated brain extraction.** *Hum Brain Mapp* 2002;17:143–55 CrossRef Medline
19. Zhang Y, Brady M, Smith S. **Segmentation of brain MR images through a hidden Markov random field model and the expectation-**

maximization algorithm. *IEEE Trans Med Imaging* 2001;20:45–57 CrossRef Medline
20. Harper CG, Kril JJ, Daly JM. **The specific gravity of the brains of alcoholic and control patients: a pathological study.** *Br J Addict* 1987;82:1349–54 CrossRef Medline
21. Gibson E, Gao F, Black SE, et al. **Automatic segmentation of white matter hyperintensities in the elderly using FLAIR images at 3T.** *J Magn Reson* 2010;31:1311–22 CrossRef Medline
22. Wu WC, Mazaheri Y, Wong EC. **The effects of flow dispersion and cardiac pulsation in arterial spin labeling.** *IEEE Trans Med Imaging* 2007;26:84–92 CrossRef Medline
23. Buxton RB, Frank LR, Wong EC, et al. **A general kinetic model for quantitative perfusion imaging with arterial spin labeling.** *Magn Reson Med* 1998;40:383–96 CrossRef Medline
24. Bokkers RP, van der Worp HB, Mali WP, et al. **Noninvasive MR imaging of cerebral perfusion in patients with a carotid artery stenosis.** *Neurology* 2009;73:869–75 CrossRef Medline
25. MacIntosh BJ, Marquardt L, Schulz UG, et al. **Hemodynamic alterations in vertebrobasilar large artery disease assessed by arterial spin-labeling MR imaging.** *AJNR Am J Neuroradiol* 2012;33:1939–44 CrossRef Medline
26. Mutsaerts HJ, van Dalen JW, Heijtel DF, et al. **Cerebral perfusion measurements in elderly with hypertension using arterial spin labeling.** *PLoS One* 2015;10:e0133717 CrossRef Medline
27. Wu WC, Jiang SF, Yang SC, et al. **Pseudocontinuous arterial spin labeling perfusion magnetic resonance imaging: a normative study of reproducibility in the human brain.** *Neuroimage* 2011;56:1244–50 CrossRef Medline
28. Guo L, Zhang Q, Ding L, et al. **Pseudo-continuous arterial spin labeling quantifies cerebral blood flow in patients with acute ischemic stroke and chronic lacunar stroke.** *Clin Neurol Neurosurg* 2014;125:229–36 CrossRef Medline
29. Firbank MJ, He J, Blamire AM, et al. **Cerebral blood flow by arterial spin labeling in poststroke dementia.** *Neurology* 2011;76:1478–84 CrossRef Medline
30. van Es AC, van der Grond J, ten Dam VH, et al; PROSPER Study Group. **Associations between total cerebral blood flow and age related changes of the brain.** *PLoS One* 2010;5:e9825 CrossRef Medline
31. Lu H, Clingman C, Golay X, et al. **Determining the longitudinal relaxation time (T1) of blood at 3.0 Tesla.** *Magn Reson Med* 2004;52:679–82 CrossRef Medline
32. Lotz J, Meier C, Leppert A, et al. **Cardiovascular flow measurement with phase-contrast MR imaging: basic facts and implementation.** *Radiographics* 2002;22:651–71 CrossRef Medline
33. Tang C, Blatter DD, Parker DL. **Correction of partial-volume effects in phase-contrast flow measurements.** *J Magn Reson Imaging* 1995;5:175–80 CrossRef Medline
34. Wu B, Wang X, Guo J, et al. **Collateral circulation imaging: MR perfusion territory arterial spin-labeling at 3T.** *AJNR Am J Neuroradiol* 2008;29:1855–60 CrossRef Medline
35. Chen Z, Zhang X, Yuan C, et al. **Measuring the labeling efficiency of pseudocontinuous arterial spin labeling.** *Magn Reson Med* 2017;77:1841–52 CrossRef Medline